LA-UR- 11-04039

Approved for public release; distribution is unlimited.

Title:	Effects of Grain Boundary Structure and Distribution on the Spall Response of Copper
Author(s):	Juan P. Escobedo-Diaz, Darcie Dennis-Koller, Ellen K. Cerreta and Curt A. Bronkhorst
Intended for:	Publication of Proceedings Paper of Shock Compression of Condensed Matter Conference 2011, Chicago,Il.

Los Alamos
NATIONAL LABORATORY
EST.1943

Form 836 (7/06)

EFFECTS OF GRAIN BOUNDARY STRUCTURE AND DISTRIBUTION ON THE SPALL RESPONSE OF COPPER

J.P. Escobedo, D. Dennis-Koller, E.K. Cerreta and C.A. Bronkhorst

[1]MST-8, [2] WX-9, [3]T-3: Los Alamos National Laboratory, Los Alamos NM 87545

Abstract. Plate impact experiments have been carried out to examine the influence of grain boundary characteristics, i.e density and structure, on the spall response of Cu samples with grain sizes of 30, 60, 100 and 200μm. The peak compressive stress is ~1.50GPa for all experiments, low enough to cause an early stage of incipient spall damage. A clear effect of the grain size is observed in the free surface velocity behavior after the pull-back minima, when re-acceleration occurs. The post-impact metallographic analyses show that for the materials with intermediate grain sizes (60μm), the damage behavior is dominated by the growth of isolated voids and plastic dissipation. Whereas in the 30 and 200μm samples, void coalescence is observed to dominate the damage behavior. Electron backscatter diffraction (EBSD) observations show that special boundaries corresponding to Σ3-type (~ 60° <111> misorientation) are more resistant to void formation.

Keywords: Copper, spall, microstructure.
PACS: 47.40.-x, 47.40.Nm.

INTRODUCTION

An extensive body of literature exists regarding the effect of the microstructure on the spall response of materials. The pioneering studies on this subject date back to the classical works by Seaman and Curran [1,2]. However, most of the cited and subsequent work has primarily focused on the effects of microstructure on pull-back measurements in experiments in which the sample experienced complete failure. In this scenario, many parameters and mechanisms (i.e. shock hardening, void nucleation, growth and coalescence) are intertwined. This precludes any significant conclusion about the individual contributions of material characteristics and kinetics of loading from these measurements.

Moreover, the evolution of plastic processes leading to incipient cracking or void formation in a material has not been fully addressed. To accurately predict dynamic failure of high purity metals, it is necessary to track the microstructural evolution of plasticity leading to early stage damage. This is the main objective addressed in this study: to elucidate fundamental mechanisms of void nucleation, growth, and coalescence for specific microstructural details. For this purpose, incipient spall experiments are performed on high-purity copper samples with a known grain boundary density/distribution (grain size) to examine the relationship between these defect characteristics and void growth.

EXPERIMENTAL PROCEDURE

All target materials were prepared from fully annealed 99.999% pure oxygen-free high-conductivity (OFHC) copper. The samples have average grain sizes of 30, 60, 100 and 200μm following annealing under vacuum at 450°C for

30min., 600°C for 1hour, 850 °C for 1hour and 900°C for 35min, respectively. The results of the complete metallographic characterization have been reported elsewhere [3]. It should be noted that not only was the defect density/distribution (grain boundary) strictly controlled, but the defect nature (grain boundary type) was, as well. The fraction of boundaries with misorientations of 60°, that fulfill the special Σ3 boundary criteria, were held to a similar value of ~0.65 fraction to grain boundaries.

Plate impact experiments

Plate impact experiments have been conducted using a smooth bore 78mm light gas gun. Velocity profiles are obtained using a VISAR probe[4]. A single, well characterized loading condition is chosen for all experiments to ensure the kinetic aspects of the tensile stress profile evolution remain consistent for all experiments. Quartz impactors (z-cut, 2mm nominal thickness) are mounted on Lexan sabots and launched using Ar gas. The use of Quartz impactors ensures that a single, elastic shock wave is produced in the stress range of interest to this study. Table I lists the experimental details and the calculated values from the free surface velocity traces.

RESULTS AND DISCUSSION

As listed in Table I, a significant effect of the grain size on the measured spall strength for the current loading conditions and microstructures was not observed. However, a clear effect on the measured response in the region of the free surface velocity (FSV) after the minima is seen. Fig. 1.a shows this region. For an easier comparison, all traces were shifted so that the traces start at t = 0. As it has been reported [3,5], the free surface velocity behavior in this region serves as the best indicator of the active mechanism of damage evolution occurring in the sample. It is observed that the 30 and 200μm samples exhibit a monotonic rise from the minima to the spall peak, while the intermediate grain sized samples, 60 and 100μm, showed a slower rate suggesting a difference in damage behavior. For the present discussion, only the two extreme cases are addressed: the responses of the 60 and 200μm samples.

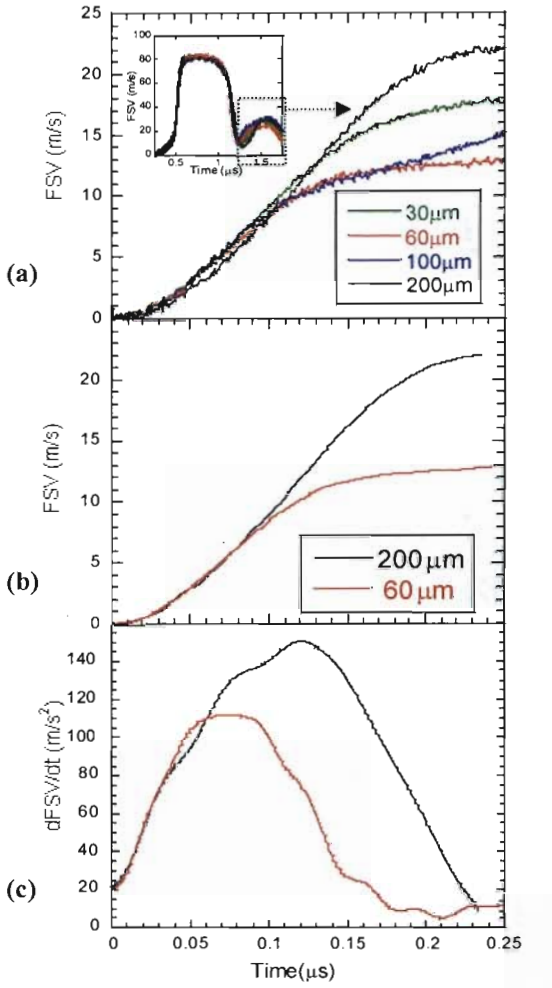

Figure 1. (a) Free surface velocity traces after the minima. (b) smoothed using a FFT filter, (c) time derivative.

In ductile materials, the rate at which the velocity rises after the minima is generally related to the void growth rate (V_v) in the following form [3]:

$$\frac{dFSV}{dt} = A\left(\dot{V}_v - B\right) \qquad (1)$$

where A and B are proportionality constants.

TABLE 1. Experimental configurations and measured properties for plate impact experiments

Exp. No	g.s μm	Target th, mm	Vp, m/s	σ_{comp} GPa	σ_{spall} GPa	V_{sp-pk} m/s	Void %	Void ave μm
1	30	3.998	134	1.50	1.38	18	0.496	38
2	60	4.030	133	1.50	1.36	14	0.249	23
3	100	4.037	131	1.46	1.31	17	0.416	33
4	200	3.899	131	1.46	1.38	22	0.507	55

Note: For all experiments 2.02mm-thick z-quartz flyers were used.

Thus, the rate of damage can be correlated to the instantaneous acceleration of the free surface velocity at a given time. Due to the noise inherent to the measurements, a fast fourier transform filter was applied to the raw data of the selected traces (60 and 200μm) to avoid any artifacts in our analyses. The results of the smoothing operation are shown in Fig 1.b. From these processed traces, a calculation of the time derivative was performed and the results are shown in Fig 1.c. It is observed that the 60μm shows an early decrease in the acceleration with respect to the 200μm sample, indicating a higher resistance or hindrance to damage growth. Given that the only variable in these experiments is the grain boundary density and distribution, the acceleration behavior, and inherently the damage behavior, must then be associated to the differences in grain boundary

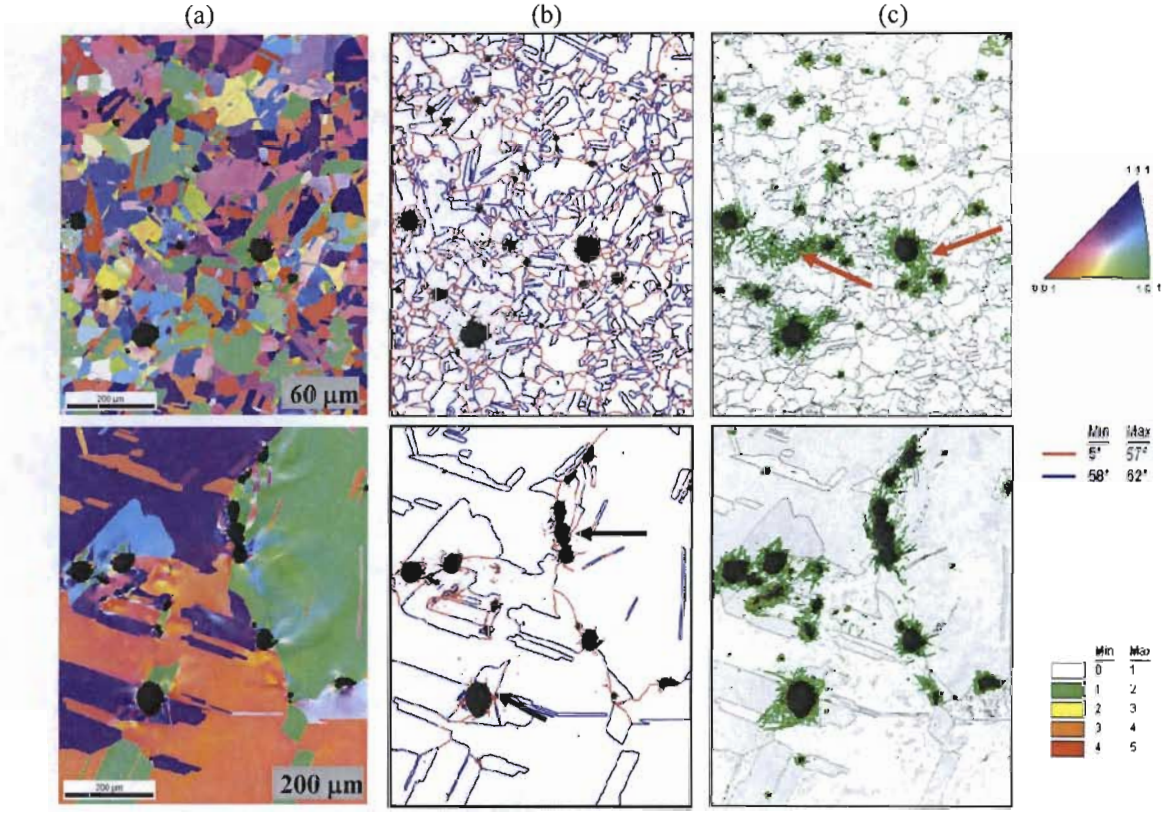

Figure 2 EBSD Maps (a) orientation, (b) grain boundary, (c) kernel average misorientation

characteristics.

Fig 2.a shows orientation maps of areas containing damage in the form of voids. As expected, most of the damage occurs at the grain boundaries. Due to the predominant presence of Σ3-type of grain boundaries, the overall distribution can be partitioned into Σ3 (or 60° misorientation about the <111> axis) and non-Σ3 (<60°) type of grain boundaries. Fig 2.b shows the boundary maps of the same regions, it is observed, in both cases, that the damage developed preferentially along non-Σ3 type grain boundaries (colored red). Results that indicate that the structure of the grain boundary determines the preferred location for void nucleation.

Fig. 2b also shows different void morphology and size for these two samples. As listed in Table I, the total damage content and void size average is larger in the 200μm case. These differences result from the interaction between nucleated voids. While in the 60μm sample, there is predominantly individual void growth, in the 200μm sample more coalescence, as indicated by the arrows, is observed. The void interaction behavior can then be related with the spatial distribution of the grain boundaries.

Fig. 2.c shows the average kernel misorientation maps of the selected areas. This measurement is an approach generally used to correlate plastic deformation to a microstructural misorientation. The misorientation map for the 200μm specimen shows highly localized deformation fields around the already coalesced voids, while the 60μm sample shows zones of relatively high misorientation linking voids (arrows), which have not yet coalesced. A result that suggests that some of the energy supplied by the shock could have been dissipated by a remote plastic work and resulted in a higher misorientation tracked in this measurement.

These observations confirm the inferences drawn from the acceleration rates shown in Fig. 1c. Those with more remote plastic dissipation loss (60 μm) will have a lower damage growth rate and a, consequently, lower acceleration in the free surface velocity rate. On the contrary, in the case where plastic flow localizes around the growing voids, i.e. coalescence, most of the driving energy is spent in void growth to cause a very rapid damage growth, in turn, accelerating the rate of the free surface velocity, as observed in Fig. 1.c for the case of the 200μm sample.

CONCLUSIONS

EBSD measurements revealed that damage occurs at locations determined by the structure of the grain boundaries, in this case, non-Σ3 type. In addition, it was shown that the free surface velocity history after the pullback minima provides a direct indicator of the active mechanism of damage evolution. The damage can be characterized as a competition between void growth and plastic dissipation processes. Its behavior is dictated by the spatial distribution of the grain boundaries, inherently determined by the grain size. For the cases in which the spatial distribution of nucleated voids promotes remote plastic dissipation, there is a hindering of the damage growth rate, in turn causing a decrease in acceleration of the free surface velocity. On the contrary, in cases in which coalescence is predominant, the overall damage growth rate increases, causing higher accelerations to the spall peak.

ACKNOWLEDGEMENTS

Funding was provided by the LDRD Grant 20100006. The authors thank John Bingert for providing valuable comments.

REFERENCES

1. L. Seaman, D. R. Curran and D. A. Shockey, J Appl Phys **47** (11), 4814-4826 (1976).
2. D. R. Curran, L. Seaman and D. A. Shockey, Phys Today **30** (1), 46 (1977).
3. J.P. Escobedo et al, Journal of Applied Physics Vol. 110, 0135-- (2011)
4. Hollenback, R. E., Journal of Applied Physics 43, 4669, (1972)
5. J.P. Escobedo et al, Journal of Applied Physics Vol. 107, 123502 (2010).